Specific Aims

Ovarian cancer kills more than 14,000 women annually in the United States and brings an annual economic burden of $612 million in the United States, alone. Currently, there are no recommended screening tests for ovarian cancer and the efficacy of screening is yet to be demonstrated in clinical trials[1]. Further, the cancer is most often diagnosed at stage III (59%) or stage IV (29%) resulting in 5-year survival rates of 42% and 26%, respectively[2]. Current treatment methods involve chemotherapy or radiation that have severe adverse health effects. Thus, the development of a more potent, targeted therapeutic option is critical. We aim to develop an ovarian cancer-specific nanoparticle-based diagnostic and therapeutic delivery system that will overcome limitations of current drug therapies and reduce unintended side effects.

Aim #1: Design and selection for liposomal carrier and drug nanoparticle. We will select for attributes that are known to enhance nanoparticle (NP) stability and take advantage of the enhanced permeability and retention effect (EPR) present in tumor microenvironments. Most therapeutic liposomal carriers are designed to have 100 to 200 nanometers (nm) diameters[3] making them large enough to selectively go through large fenestrations present in malformed tumor blood vessels unique to tumor microenvironments[4]. However, the EPR effect may not be present in all tumors[5]. We aim to account for this by selecting for a diameter that is small enough to allow for the liposomal carrier to reach all cell types where active selection will be the primary form of selection but that is large enough such that it will show a probabilistic preference for tumor microenvironments if the EPR effect is present. Additionally, we aim to design a potent drug nanoparticle that will self-assemble into a compact spherical shape to allow for dense packing of drug nanoparticle inside the liposome. These properties combined with active ligand-targeted selection will make for a highly selective and potent drug.

Aim #2: High-throughput screening to generate ovarian tumor-specific aptamers. Transcriptomic and proteomic data will be used to identify differentially expressed surface markers that are upregulated in ovarian cancer cell lines and tumors. Based on preliminary data and previous work, MUC16 (CA125) and CD151, were selected as the target surface receptors. Predicted conformations and binding affinities of ~10^7 ssDNA aptamers will be calculated using molecular folding and docking algorithms. The aptamers will be ranked from greatest to least binding affinity for the two selected surface receptors, and the top 100,000 will be tested using an adapted version of the Systematic Evolution of Ligands by Exponential Enrichment (SELEX) approach. Briefly, a synthetic library of aptamers will be incubated with the NIH:OVCAR3 cell line and HEK293Ts for positive and negative selection, respectively. The supernatant will be collected and analyzed using next-generation sequencing to determine which aptamers are internalized. RT-qPCR for the constant regions of the aptamers will determine relative uptake by each cell line. This process will be continued until 5 aptamers have been identified for each target receptor (10 total).

Aim #3: Synthesizing PEG-coated, surface charge switchable, drug nanoparticle incorporated liposome. The selected aptamer will be conjugated to a lipid molecule to generate the drug-incorporated liposome. The polyFdU-prodrug nanoparticle will be synthesized by the self-assembly of polyFdU and cisplatin prodrug. PolyFdU will be synthesized by TdT-catalyzed polymerization, followed by incorporating a single amino-ddUTP (5-Propargylamino-2',3'-dideoxyuridine-5'-triphosphate) by TdT. The cisplatin prodrug will be conjugated onto the polyFdU chain by EDC/NHS chemistry, resulting in a hydrophobic tail to drive self-assembly. The liposomes will be formed using HSPC (hydrogenated soy phosphatidyl choline), cholesterol, MPEG-DSPE (methoxypoly-(ethylene glycol)-distearoyl-phosphatidyl-ethanolamine), and MalPEG (maleimide-terminated PEG-DSPE). To increase liposome uptake, zwitterionic lipids will be incorporated into liposome. The pre-synthesized aptamer-lipid conjugates and dual-drug nanoparticles will be mixed with the liposome solution during the hydration step. The size of the liposome will be characterized by dynamic light scattering, the morphology of the liposome will be characterized by TEM, and the drug nanoparticle loading as well as leakiness of the liposome will be analyzed by fluorescent imaging.

Aim #4: In vitro and in vivo testing for optimal nanoparticle delivery systems. In vivo and in vitro tests will be conducted to determine the specificity and efficacy of the fluorescently-labeled prodrug NP. For in vitro studies, fluorescence and cell death will be the primary measured outputs and the testing groups will be ovarian cancer, non-ovarian cancer, and healthy fibroblast cell lines. First, the prodrug NP will be introduced to a static 2D culture to determine its ability to successfully penetrate the cell. After, the assays will be repeated with 3D cultures of ex vivo tumors to determine specificity and the ability to deliver the aptamer payload to a therapeutic level. Fluorescently-labeled blank NPs, and liposomes with or without cisplatin, will act as controls. Next, microfluidic devices containing cells from the abovementioned groups in connected chips, or an ovary on a chip model[42] connected to a tumor on a chip will be used to assess the prodrug NP's effect on tumor size. Finally, the in vivo testing phase will consist of mice with ovarian cancer, non-ovarian cancer, and healthy mice. Tumor size, fluorescence in tissue and interstitial fluid, and serum antibody levels will be analyzed.

Significance and Background:

Ovarian cancer is responsible for 5% of all female cancer deaths in the United States and at least 22,000 new cases are diagnosed annually in the United States (US)[1]. Worldwide, nearly 300,000 women are diagnosed with the cancer every year leading to significant health and financial stress on the patient in addition to a severe economic burden totaling more than $600 million in the US. Currently, there are no recommended screening tests for ovarian cancer and the efficacy of screening is yet to be demonstrated in clinical trials[1]. Further, the cancer is most often diagnosed at stage III (59%) or stage IV (29%) resulting in 5-year survival rates of 42% and 26%, respectively[2]. Current treatment methods involve intravenous or intraperitoneal chemotherapy with a combination of cisplatin and one of 12 other drugs. Both treatment methods have severe short-term and long-term side effects, including increased risk for infection and kidney damage, respectively. Thus, a more targeted, potent treatment is necessary to improve survival rates and decrease adverse health effects. To this end, we aim to develop a self-assembling drug-conjugated nanoparticle that is enveloped by an aptamer-coated liposome such that the ovarian cancer cells can be specifically targeted and receive a high dose of drug. We propose to accomplish this in three phases: (i) in silico aptamer design and liposome optimization, (ii) in vitro selection of aptamers and nanoparticle assembly, and (iii) efficacy testing in cell cultures and murine models of ovarian cancer.

Innovation:

Many of the current nanoparticle therapeutics used as treatments for cancer are heavily reliant on the presence of abnormal vasculature near tumor microenvironments. Most commercially available nanoparticle therapeutics have diameters between 100 to 200 nms[3] which only allow them to selectively enter through large fenestrations present in blood vessels unique to tumors[4]. These fenestrations however are not present in all tumors thus limiting efficacy of treatment[5]. A pre-administrative screen can be used to identify patients who show signs of the EPR effect, but this increases time and cost of diagnoses[6]. We aim to overcome this by designing our liposomal carrier to be slightly smaller than the lower effective limit such that it is internalized by all cell types but large enough such that it increases resistance in healthy tissues. Thus, the liposomal carrier will be more likely to choose the path of least resistance and be taken up by tumor cells. Additionally, we aim to select for conditions so that the drug nanoparticle self assembles into a compact spherical shape.

Previously used aptamer libraries consist of ~10^{14} random nucleotide sequences, which requires many cycles of SELEX as most aptamers will not be specific for the intended use. We aim to harness genomic data in combination with computational modeling systems, to generate a targeted library of sequences that demonstrate high affinity to specific surface receptors[17,18,20-24]. This will decrease the number of selection cycles and the abundance of non-specific aptamers in a high throughput manner[24-26]. Additionally, liposomes have been shown to increase the circulation time of aptamers thereby enhancing the efficiency of drug delivery[27].

It was shown that 5'-fluorouracil and cisplatin have synergistic effects for the treatment of ovarian cancer[28]. Thus, we hypothesize the combination of these two drugs in the same drug carrier will achieve high potency and decrease drug-resistance. However, small molecules are more prone to leak out of the liposomes, leading to toxicity to normal tissue. Thus, we propose a dual-drug nanoparticle that consists of two components, which has high drug-loading efficiency and is less likely to leak out. Firstly, FdUTP and FdUMP are metabolic intermediates of 5'-fluorouracil, so we have selected polyFdU instead of 5'-fluorouracil to have the same drug effect. polyFdU with different lengths can be easily obtained by TdT-catalyzed polymerization, an enzyme that is able to polymerize even unnatural nucleotides without template[29]. Secondly, a prodrug of cisplatin has been studied, which is less toxic and can drive self-assembly by its hydrophobic tail[30].

Liposomes are a popular drug delivery method due to biocompatibility and low toxicity. However, bare liposomes also suffer from relatively rapid clearance because of recognition by immune system as non-self. By coating nanoparticles or liposomes with polyethylene glycol (PEG), it is possible to create "stealth" brushes that mimic a cell's glycocalyx thereby delaying immune clearance[31-33]. Although liposomes can accumulate to tumor microenvironment with the help of EPR effect and aptamer targeting effect, the internalization of the drug vehicle is a challenge. Previous work has shown that cationic surface enhances the internalization of nanoparticles into cells, but that the cationic property can increase immunogenecitiy[34]. Thus, we will utilize zwitterionic polymers. The zwitterionic polymer is neutral to negatively charged overall in physiological conditions, of which the pH is higher than pKa of the zwitterionic polymer. As a result, the nanoparticles will show prolonged circulation time. After accumulating in the relatively acidic tumor tissue, due to the intrinsic pH differences between various solid tumors (~6.8) to that of blood or normal tissues (~7.4), the zwitterionic polymer-based nanoparticles changed to be positively charged, which facilitates the cellular uptake[35].

In vitro and in vivo efficacy testing workflows have been well established[41]. However, the use of microfluidic devices is still new. Other groups have worked to develop disease and organ models, either in complex, or minimized form. A recently developed ovary on a chip model by Nagashima et al. has the ability to secrete hormones and form oocytes[42]. Linking this model to a tumor on a chip model would allow us to see the effect on tumors on normal ovarian function and provide a more robust testing model.

Approach:

Aim #1: Design and selection for liposomal carrier and drug nanoparticle

Phase 1: Selection of Size, Shape, Physical and Chemical Properties of the Liposomal Drug Carrier. We aim to design, produce and generate a ligand-targeted liposomal carrier that is stable during circulation and that exploits the enhanced permeability and retention (EPR) present in tumor microenvironments[4]. This combination will greatly increase efficacy and reduce toxicities associated with free-administration of drug nanoparticles via three methods: active targeting[8], the EPR effect[4], and increased circulation times[7]. The EPR effect exists in certain tumor microenvironments as a result of tumoral angiogenesis triggered by hypoxia and the lack of effective lymphatic vasculature[8]. The release of angiogenic factors in response to hypoxia in tumors lead to the formation of abnormal blood vessels near the tumor microenvironments which lack smooth muscle, have wider lumens, and have larger fenestrations[7,8]. Large nanoparticles (NPs) are selectively uptaken into the interstitial space of the tumor microenvironment due to the large fenestrations present in the malformed blood vessels[4], allowing for molecules up to 500nm in diameter to go through[7]. Additionally, tumors lack effective lymphatic vasculature which lead to diminished clearance[7,8], thus enabling for the accumulation of these NPs in cancer cells. We will exploit this effect as a secondary selection strategy by designing the liposomal carrier to be small enough to reach all cell types with some resistance so that it will preferentially target tumor microenvironments if malformed blood vessels do form. Most therapeutic NPs that selectively rely on the EPR effect range in diameters between 100-200 nm[3]. To implement this quasi-selective strategy, we will select for our liposomal carrier to be slightly below the lower size limit of the 50 nms[7]. Additionally, this reduced diameter size should give our NP added systemic circulation time[7,8,10], lead to less recognition by the mononuclear phagocyte system (MPS)[10,] and lead to less capturing by the RES[10] allowing for higher concentrations of the drug nanoparticle to make its way into the cytoplasm cancer cell.

Additional selection will take place to select for factors known to decrease immunogenicity and enhance stability. The reduced diameter size already accomplishes some of this desired effect but surface potential, zeta potential and shape also play pertinent roles in immunogenicity and stability. NPs with high magnitude surface potentials and zeta potentials[9] are more stable during blood flow since they tend to not agglomerate and have chemical properties that allow for enhanced blood flow solubility. NPs with positive zeta potentials and that have high surface hydrophobicity are easily recognized by the MPS system thus NPs with negative zeta potentials and high surface potentials will be selected for[10]. **Intended outcome: To take advantage of these properties we aim to implement a liposomal carrier having a 40 nm diameter, zeta potential greater than -50mV, surface potential greater than |30| mV.**

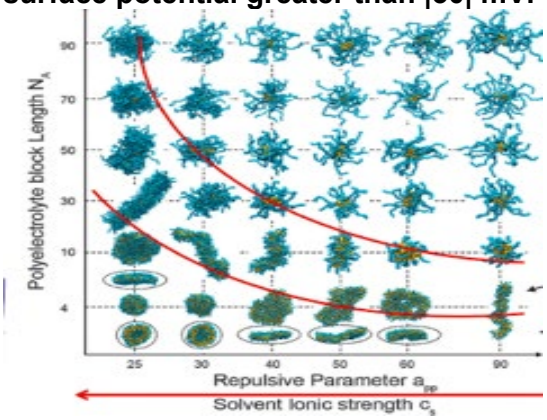

Figure 1. Shape trend[11]. General trend as to how shape changes with ionic strength and length. As length of hydrophilic chain gets smaller and ionic strength gets stronger, compact spherical formation is achieved.

Phase 2: Conditions Required for Self-Assemblage of a Compact Spherical-Shaped Drug Nanoparticle. Previous studies show that the most pertinent factors affecting the self-assemblage of the drug nanoparticle are the length of its hydrophilic chain and the ionic strength of the solvent[11]. To allow for dense fitting of the drug nanoparticle inside of the liposomal carrier, the chain length and ionic concentrations were selected such that to drug nanoparticle self-assembles into a compact spherical micelle. A poly-FdU chain of 54 nucleotides placed in a solution with high ionic strength (>.01M NaCl) has been shown to self-assemble in a spherical shape[10]. We plan on building on this model, and to ensure for proper self-assemblage at the slight expense of compactness, a slightly larger nucleotide length will be chosen.

Intended outcome: Implement a 58-nucleotide hydrophilic chain placed in a .04 M NaCl solution for the compact spherical formation of the drug nanoparticle.

Aim #2: High-throughput screening to generate ovarian tumor-specific aptamers.

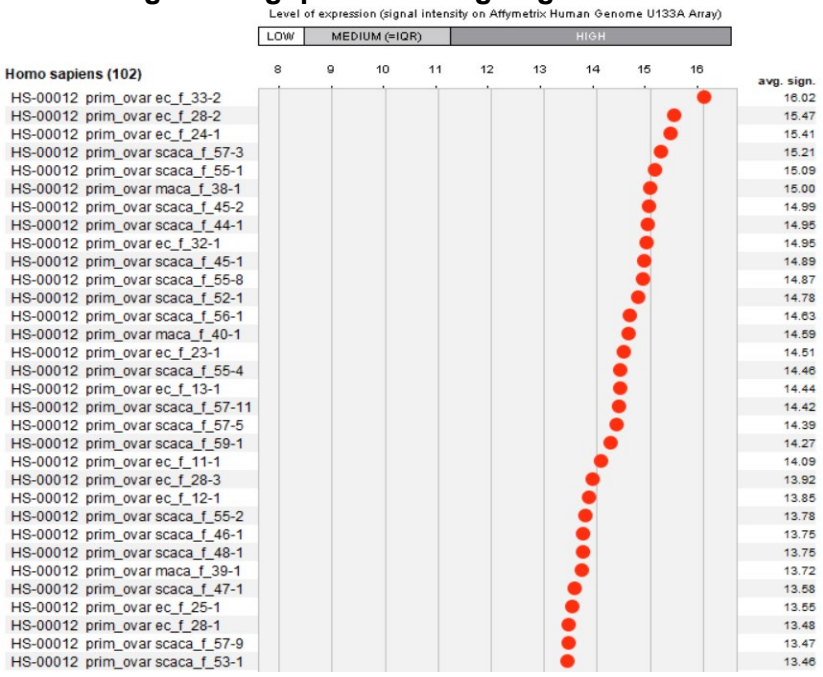

Figure 2. Expression of MUC16 in primary ovarian cancer tumor biopsies. Level of expression determined from signal intensity on Affymetrix Human Genome U133A Array (n = 102 samples). Higher intensity indicates greater gene expression.

Phase I: Generation of Targeted Aptamer Library. The targeted aptamer library will be generated by analyzing the transcriptomic and proteomic data sets for 888 ovarian tumor biopsy samples, including samples from Stages I-IV and varied genetic backgrounds, and data sets for 58 ovarian cancer cell lines, to determine unique differentially expressed genes that are upregulated in ovarian cancers[12]. Previous work has identified two transmembrane proteins, MUC16 (CA125), and CD151, as reliable biomarkers for ovarian cancer, whose expression levels correlate with prognosis[13–16]. In agreement, preliminary analysis of transcriptome data also produced MUC16 as significantly upregulated in ovarian cancer as compared to other types of cancer and healthy tissues (Figure 2).

A random library of single-stranded DNA (ssDNA) aptamers (~10^7 sequences) will be generated for each target, comprised of a 20-nucleotide variable sequence – shown to be more effective than longer versions[17]– that is flanked on both sides by a constant 30 nucleotide sequence. By using ssDNA aptamers, rather than RNA aptamers, we will avoid potential PCR bias in the initial libraries and the aptamers will be more stable. Once designed, the 3-D conformations of the ssDNA will be predicted using a command line version of an established protocol[18,19]. Briefly, the DNA secondary structure is generated using the program Mfold, then constructed and translated into the 3D structure using Assemble2, Chimera, and VMD, and then refined to the final structure using VMD[18]. This workflow consists of identifying the conformation with the lowest Gibb's free energy out of all possible conformations of the molecule. Next, using the known structure of the surface receptor, the binding affinity of each aptamer to each target will be calculated using Proteotronics, software which was previously shown to predict affinities in agreement with experimental data[20], to estimate binding affinity. The aptamers will be ranked from greatest to least binding affinity and the top 10,000 aptamers will be moved to the next stage.

We hypothesize this workflow will enable the identification of target-specific aptamers. The main challenge facing this approach is accurately predicting the binding affinities between aptamers and targets. Recently developed multilevel workflows that incorporate 2-D and 3-D structure were demonstrated to accurately predict structures in the Nucleic Acid Database and Protein Data Bank databases[18]. Additionally, generalized regression neural networks based on quantitative structure-activity/property relationships predicted aptamer binding affinities that showed correlation coefficients to known binding affinity values of influenza virus of 0.889 and 0.892 for trained and untrained datasets, respectively, suggesting these methods and others being developed are accurate and can be used for predictive modeling[20-24]. **Intended outcome: Targeted aptamer libraries for two surface receptors specific to ovarian cancer (MUC16 and CD151).**

Phase II: High-Throughput Identification of Ovarian Cancer-Specific Aptamers. Using the targeted aptamer library (Phase I), High-Throughput Cell Internalizing SELEX (HC-SELEX) will be utilized to identify five ovarian cancer-specific aptamers. By incorporating both positive and negative selection with next-generation sequencing, the number of cycles of SELEX can be reduced to less than 15[17,24,25]. Briefly, the aptamer library will be incubated with the NIH:OVCAR3 cell line, a fully characterized ovarian cancer cell line, followed by washing with salt detergents to remove weak-binding aptamers from the cells. Next, the supernatant is collected, filtered through a streptavidin column to remove dsDNA, PCR amplified, and then Illumina adapters are added, followed by 2x150 bp PE sequencing with minimum of 500X coverage to ensure the full 90 nucleotide aptamer can be identified. The cells are harvested to quantify the abundance of internalized aptamers via RT-qPCR with

primers that match the constant regions of the aptamers. Then the ratio of internalized aptamers to aptamer library size can be calculated to estimate the overall efficiency of the library.

In parallel, a similar workflow is performed with a non-cancerous cell line, HEK293Ts, which has been used previously in SELEX procedures[17,25,26]. The aptamer sequences that drop out of the positive selection screen were internalized by the ovarian cancer cell line, and thus are potential candidates, whereas the sequences that drop out of the negative selection were internalized by the HEK293T cells, and thus, are not specific to ovarian cancer, and are removed from the aptamer library. If a much greater quantity of aptamers is internalized by the HEK 293Ts, a new target receptor will be selected. The HC-SELEX process is repeated with decreasing aptamer incubation time for positive selection and increasing incubation times for negative selection until 5 aptamers have been identified. By reducing the incubation time, only the aptamers with the highest binding affinity will be able to be internalized by the ovarian cells, while increasing incubation time with the HEK293Ts will allow non-specific aptamers more time to be internalized, thus removing them from the potential candidate list. **Intended outcome: 5 aptamers unique to each surface receptor (10 total).**

Aim #3: Synthesizing PEG-coated, surface charge switchable, drug nanoparticle incorporated liposome.

To generate the drug-incorporated liposome, first, the selected aptamer is conjugated to a lipid molecule allowing it to be inserted into the liposome. A method developed by Chan et al. involving a lipid phosphoramidite intermediate will be utilized[36]. Next, the polyFdU-prodrug nanoparticle is synthesized. PolyFdU can be synthesized by TdT-catalyzed polymerization on a single-stranded oligoT stand[29]. Then an amino group can be introduced onto the tail of polyFdU by incorporating a single Amino-ddUTP (5-Propargylamino-2',3'-dideoxyuridine-5'-triphosphate) by TdT. Then the carboxyl-group-containing cisplatin prodrug can be conjugated onto the polyFdU chain by EDC/NHS chemistry, resulting in a hydrophobic tail on the hydrophilic polyFdU chain. Under certain lengths of polyFdU and certain salt concentrations, the amphiphilic molecule can drive self-assembly and form nanoparticles.

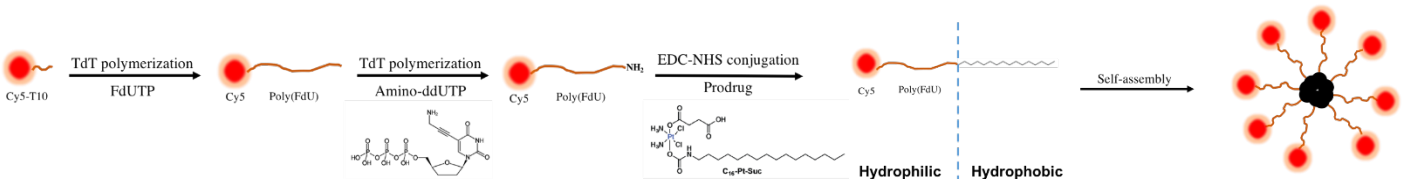

Figure 2. Scheme for the formation of self-assembled dual-drug nanoparticles

The liposomes will be formed using standard protocols. Briefly, we will use HSPC (hydrogenated soy phosphatidyl choline), cholesterol, MPEG-DSPE (methoxypoly-(ethylene glycol)-distearoyl-phosphatidyl-ethanolamine), and MalPEG (maleimide-terminated PEG-DSPE) as raw materials[37]. To increase liposome uptake, zwitterionic lipids (1,2-dioleoyl-snglycero-3-phosphocholine (DOPC) or 1,2-dioleoyl-sn-glycero-3-phosphoethanolamine (DOPE)) will also be incorporated into liposome to obtain the PEG-coated, surface charge switchable liposome[35, 38]. Then the pre-synthesized aptamer-lipid conjugates and dual-drug nanoparticles will be mixed with the liposome solution during the hydration step[37, 39, 40].

If the in vitro data shows insufficient uptake because PEG shields all the positive charges, a breakable PEG linker can be incorporated such that under tumor microenvironment conditions, the PEG molecules break off and reveal the positive charge[35]. Further, if the liposome shows poor intracellular lysosomal escape, pH-sensitive liposomes present an alternative, of which the pH sensitive component undergoes local membrane destabilization that allows for drug efflux from the liposome into surroundings[35].

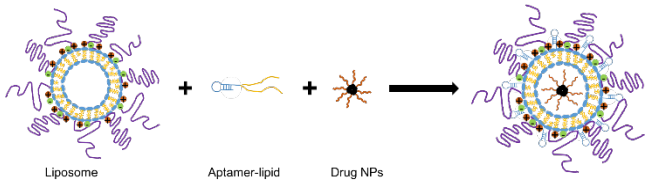

Figure 3. Formation of surface charge switchable liposome with aptamers on the surface and drug NPs inside.

Finally, the size of the liposomes will be characterized by dynamic light scattering (DLS). Electrophoresis will be done to select for liposomes with specific zeta potential that is chosen in Aim #1. The morphology of the liposome can be characterized by microscopies (TEM, AFM, etc.) as well as fluorescent imaging. The 5' end of

aptamer can be tagged with a fluorophore, and the 5' end of polyFdU chain can be tagged with a second fluorophore. Fluorescent imaging can also verify if the drug nanoparticles were incorporated into the liposomes. In addition, the half-life and leakiness of liposomes will be tested by incubating them in physiological solution and imaging them after certain amount of time (1h, 6h, 24h, 48h, and 72h). **Intended outcome: Obtain aptamer-lipid conjugates, dual-drug nanoparticle, and surface charge switchable liposome with aptamers on the surface and drug NPs inside. The drug NPs should be stable inside liposome for at least 24h under physiological condition.**

Aim #4: In vitro and in vivo testing for optimal nanoparticle delivery systems.

Efficacy testing will be split into in vitro and in vivo testing phases. For both phases, the control groups will be fluorescently-labeled blank NPs, and fluorescently-labeled liposomes with or without cisplatin. The prodrug NP will be similarly labelled.

Phase I: In vitro testing. Ovarian target cell lines, non-ovarian cancer cell lines, and normal non-cancerous cell lines will be used first in a static 2D culture for high throughput screening to determine the specificity and efficacy of the prodrug NP. The prodrug NPs and controls will be introduced into the cell culture medium at various concentrations and sampled at several time points, after which fluorescence, cell viability, and cisplatin concentration will be measured both in the cells and in the media. This will serve to inform NP specificity, NP uptake efficiency by the cells, and will assist in dosage calculations for downstream testing. Off target effects will be assessed in the relative cell death of non-ovarian cancer, and normal cells compared to ovarian cancer cells. If relative cell death exceeds 20%, reassessment of the carrier system to increase specificity will be required.

The process will be repeated with 3D cultures of ex vivo tumors of ovarian cancer, non-ovarian cancer, and tissue slices of non-cancerous tissue. Ex vivo tumors are preferred over cultured tumors as there are no size limitations and offer better comparisons intercellular communication and morphology than cultured organoids[41]. Tissues will be sectioned to assess NP tumor penetration depth via fluorescence and intercellular communication, ECM, and spatial organization of the cells are introduced as factors to be considered. Real-time fluorescence imaging of ex vivo tissues will be used to track tumor size in addition to depth penetration via sectioning.

Next microfluidic devices will be used with the three same–cell types in a series of chips, and with a recently developed ovary on a chip model[42] connected to a tumor on a chip. Interstitial fluid flow will be used to more accurately model diffusion of the NPs into the tumor from vasculature. The effect of the tumor microenvironment and high amounts of hormones in the ovaries on NP uptake efficiency and NP degradation can be more accurately assessed. Real time fluorescence imaging will once again be used to track tumor size. Circulating fluid will be regularly sampled for cisplatin and NP concentration to determine uptake efficiency, NP degradation (half-life) and clearance. A drawback platform is the limitation on size. However, understanding the effects of vasculature flow dynamics, and ability to precisely locate fluid channels and control permeability with various filter sizes far outweigh the limitations**.** The microfluidic chips can be used to predict dosage with greater accuracy, for in vivo testing based on half-life results, a better test than static half-life tests in serum which do not account for the effect of cell secreted molecules, protein/NP interactions, and fluid flow on NP stability. Success criteria will be high specificity and low toxicity: high ovarian cancer cell death/tumor size reduction and little effect on non-cancerous cells, a half-life greater than 1 hour to allow for sufficient circulation in vivo and uptake by the tumor.

Phase II: In vivo testing. Murine models will be used for in vivo testing as they are a well-established, well characterized model[43]. Humanized female mice with intrabursal human tumor xenografts in a single ovary, mice with a subcutaneous xenograft, and healthy cancer-free mice, will be administered varying doses two weeks post-xenograft. Tumors will be measured before each drug/control injection with ultrasound. The prodrug NPs and controls will be introduced intravenous or intraperitoneal injection as is the current standard in ovarian cancer therapy. Pharmacokinetics such as NP uptake, biodistribution, clearance, absorption will be assessed through NIR imaging (fluorescence) and blood/intraperitoneal/intrabursal interstitial fluid for NP concentrations, and blood/urine samples for clearance[44]. In vivo half-life of the NP will be assessed after determining the appropriate dose via tracking blood/intraperitoneal NP concentration. Immunogenicity of the NP will be assessed through analyzing serum antibody levels. Metabolic profiling will also be used to assess efficacy of the treatment and off target tissue damage. Success criteria will include low NP-specific serum antibody levels, ovarian tumor size reduction, little off target tissue damage (especially that of kidney and liver, the main site of NP degradation and clearance). **Intended outcomes: gain specificity, pharmacodynamic, and pharmacokinetic information of the prodrug NP. The NP should cause a reduction in tumor size with comparatively fewer side-effects than the liposomal cisplatin**.

References:

[1] “Worldwide Cancer Data.” *World Cancer Research Fund*, 6 Aug. 2018, https://www.wcrf.org/dietandcancer/cancer-trends/worldwide-cancer-data.

[2] Torre, Lindsey A., et al. “Ovarian Cancer Statistics, 2018.” *CA: A Cancer Journal for Clinicians*, vol. 68, no. 4, 2018, pp. 284–96. *Wiley Online Library*, doi:10.3322/caac.21456.

[3] Brown S, Khan DR. The treatment of breast cancer using liposome technology. J Drug Deliv. 2012;2012:212965.

[4] Dudley, Andrew C. “Tumor endothelial cells.” *Cold Spring Harbor perspectives in medicine* vol. 2,3 (2012): a006536. doi:10.1101/cshperspect.a006536

*[*5] Nanodrug Delivery: Is the Enhanced Permeability and Retention Effect Sufficient for Curing Cancer? Yuko Nakamura, Ai Mochida, Peter L. Choyke, and Hisataka Kobayashi. *Bioconjugate Chemistry* 2016 27 (10), 2225-2238 DOI: 10.1021/acs.bioconjchem.6b00437

[6] Greish K. (2010) Enhanced Permeability and Retention (EPR) Effect for Anticancer Nanomedicine Drug Targeting. In: Grobmyer S., Moudgil B. (eds) Cancer Nanotechnology. Methods in Molecular Biology (Methods and Protocols), vol 624. Humana Press

[7] Bozzuto, Giuseppina, and Agnese Molinari. “Liposomes as nanomedical devices.” *International journal of nanomedicine* vol. 10 975-99. 2 Feb. 2015, doi:10.2147/IJN.S68861

[8] DOMB, ABRAHAM J. *FOCAL CONTROLLED DRUG DELIVERY*. Pages 66-70. SPRINGER-VERLAG NEW YORK, 2016.

[9] Greish K. (2010) Enhanced Permeability and Retention (EPR) Effect for Anticancer Nanomedicine Drug Targeting. In: Grobmyer S., Moudgil B. (eds) Cancer Nanotechnology. Methods in Molecular Biology (Methods and Protocols), vol 624. Humana Press

[10] Immordino, Maria Laura et al. “Stealth liposomes: review of the basic science, rationale, and clinical applications, existing and potential.” *International journal of nanomedicine* vol. 1,3 (2006): 297-315.

[11] Li, Nan K., et al. “Prediction of Solvent-Induced Morphological Changes of Polyelectrolyte Diblock Copolymer Micelles.” *Soft Matter*, vol. 11, no. 42, 2015, pp. 8236–8245., doi:10.1039/c5sm01742d.

[12] Berezhnoy, Alexey, et al. “Isolation and Optimization of Murine IL-10 Receptor Blocking Oligonucleotide Aptamers Using High-Throughput Sequencing.” *Molecular Therapy*, vol. 20, no. 6, June 2012, pp. 1242–50. *PubMed Central*, doi:10.1038/mt.2012.18.

[13] Cataldo, R., et al. “A Validation Strategy for in Silico Generated Aptamers.” *Computational Biology and Chemistry*, vol. 77, Dec. 2018, pp. 123–30. *Crossref*, doi:10.1016/j.compbiolchem.2018.09.014.

[14] Domcke, Silvia, et al. “Evaluating Cell Lines as Tumour Models by Comparison of Genomic Profiles.” *Nature Communications*, vol. 4, no. 1, Dec. 2013, p. 2126. *DOI.org (Crossref)*, doi:10.1038/ncomms3126.

[15] Gedye, Craig A., et al. “Cell Surface Profiling Using High-Throughput Flow Cytometry: A Platform for Biomarker Discovery and Analysis of Cellular Heterogeneity.” *PLoS ONE*, edited by Jörg D. Hoheisel, vol. 9, no. 8, Aug. 2014, p. e105602. *DOI.org (Crossref)*, doi:10.1371/journal.pone.0105602.

[16] Hruz, Tomas, et al. “Genevestigator V3: A Reference Expression Database for the Meta-Analysis of Transcriptomes.” *Advances in Bioinformatics*, 2008, doi:10.1155/2008/420747.

[17] Jeddi, Iman, and Leonor Saiz. “Three-Dimensional Modeling of Single Stranded DNA Hairpins for Aptamer-Based Biosensors.” *Scientific Reports*, vol. 7, no. 1, Apr. 2017, p. 1178. *www.nature.com*, doi:10.1038/s41598-017-01348-5.

[18] Jiménez, José, et al. “KDEEP: Protein–Ligand Absolute Binding Affinity Prediction via 3D-Convolutional Neural Networks.” *Journal of Chemical Information and Modeling*, vol. 58, no. 2, Feb. 2018, pp. 287–96. *ACS Publications*, doi:10.1021/acs.jcim.7b00650.

[19] Koh, Judice L. Y., et al. “COLT-Cancer: Functional Genetic Screening Resource for Essential Genes in Human Cancer Cell Lines.” *Nucleic Acids Research*, vol. 40, no. Database issue, Jan. 2012, pp. D957–63. *PubMed Central*, doi:10.1093/nar/gkr959.

[20] Mallikaratchy, Prabodhika. “Evolution of Complex Target SELEX to Identify Aptamers against Mammalian Cell-Surface Antigens.” *Molecules*, vol. 22, no. 2, Jan. 2017, p. 215. *Crossref*, doi:10.3390/molecules22020215.

[21] Marcotte, Richard, et al. “Essential Gene Profiles in Breast, Pancreatic, and Ovarian Cancer Cells.” *Cancer Discovery*, vol. 2, no. 2, Feb. 2012, pp. 172–89. *Crossref*, doi:10.1158/2159-8290.CD-11-0224.

[22] Thiel, William H., Kristina W. Thiel, et al. “Cell-Internalization SELEX: Method for Identifying Cell-Internalizing RNA Aptamers for Delivering SiRNAs to Target Cells.” *Methods in Molecular Biology (Clifton, N.J.)*, vol. 1218, 2015, pp. 187–99. *PubMed Central*, doi:10.1007/978-1-4939-1538-5_11.

[23] Thiel, William H., Thomas Bair, et al. “Rapid Identification of Cell-Specific, Internalizing RNA Aptamers with Bioinformatics Analyses of a Cell-Based Aptamer Selection.” *PLoS ONE*, vol. 7, no. 9, Sept. 2012. *PubMed Central*, doi:10.1371/journal.pone.0043836.

[24] Yaseen, A., et al. “Protein Binding Affinity Prediction Using Support Vector Regression and Interfecial Features.” *2018 15th International Bhurban Conference on Applied Sciences and Technology (IBCAST)*, 2018, pp. 194–98. *IEEE Xplore*, doi:10.1109/IBCAST.2018.8312222.

[25] Yu, X., et al. “Prediction of the Binding Affinity of Aptamers against the Influenza Virus.” *SAR and QSAR in Environmental Research*, vol. 30, no. 1, Jan. 2019, pp. 51–62. *Taylor and Francis+NEJM*, doi:10.1080/1062936X.2018.1558416.

[26] Zhang, Weiwen, et al. “Prediction, Docking Study and Molecular Simulation of 3D DNA Aptamers to Their Targets of Endocrine Disrupting Chemicals.” *Journal of Biomolecular Structure and Dynamics*, Nov. 2018, pp. 1–9. *DOI.org (Crossref)*, doi:10.1080/07391102.2018.1547222.

[27] Orava, Erik W., Nenad Cicmil, and Jean Gariépy. "Delivering cargoes into cancer cells using DNA aptamers targeting internalized surface portals." Biochimica et Biophysica Acta (BBA)-Biomembranes 1798.12 (2010): 2190-2200.

[28] Scanlon, K. J., et al. "Biochemical basis for cisplatin and 5-fluorouracil synergism in human ovarian carcinoma cells." Proceedings of the National Academy of Sciences 83.23 (1986): 8923-8925.

[29] Tang, Lei, et al. "Enzymatic Polymerization of High Molecular Weight DNA Amphiphiles That Self-Assemble into Star-Like Micelles." Advanced Materials 26.19 (2014): 3050-3054.

[30] Awuah, Samuel G., et al. "A Pt (IV) pro-drug preferentially targets indoleamine-2, 3-dioxygenase, providing enhanced ovarian cancer immuno-chemotherapy." Journal of the American Chemical Society 137.47 (2015): 14854-14857.

[31] Torchilin, Vladimir P. "Recent advances with liposomes as pharmaceutical carriers." Nature reviews Drug discovery 4.2 (2005): 145.

[32] Levchenko, Tatiana S., et al. "Liposome clearance in mice: the effect of a separate and combined presence of surface charge and polymer coating." International journal of pharmaceutics 240.1-2 (2002): 95-102.

[33] Rodriguez, Pia L., et al. "Minimal" Self" peptides that inhibit phagocytic clearance and enhance delivery of nanoparticles." Science 339.6122 (2013): 971-975.

[34] Thurston, Gavin, et al. "Cationic liposomes target angiogenic endothelial cells in tumors and chronic inflammation in mice." The Journal of clinical investigation 101.7 (1998): 1401-1413.

[35] Yuan, You-Yong, et al. "Surface charge switchable nanoparticles based on zwitterionic polymer for enhanced drug delivery to tumor." Advanced materials 24.40 (2012): 5476-5480.

[36] Chan, Yee-Hung M., Bettina van Lengerich, and Steven G. Boxer. "Effects of linker sequences on vesicle fusion mediated by lipid-anchored DNA oligonucleotides." Proceedings of the National Academy of Sciences 106.4 (2009): 979-984.

[37] Cao, Zehui, et al. "Reversible cell-specific drug delivery with aptamer-functionalized liposomes." Angewandte Chemie International Edition 48.35 (2009): 6494-6498.

[38] Ahmed, Sana, Satoshi Fujita, and Kazuaki Matsumura. "Enhanced protein internalization and efficient endosomal escape using polyampholyte-modified liposomes and freeze concentration." Nanoscale 8.35 (2016): 15888-15901.

[39] áO'Donoghue, Meghan B. "A liposome-based nanostructure for aptamer directed delivery." Chemical communications 46.2 (2010): 249-251.

[40] Yoshina-Ishii, Chiaki, et al. "General method for modification of liposomes for encoded assembly on supported bilayers." Journal of the American Chemical Society 127.5 (2005): 1356-1357.

[41] Meijer, Titia G et al. "*Ex vivo* tumor culture systems for functional drug testing and therapy response prediction." *Future science OA* vol. 3,2 FSO190. 27 Mar. 2017, doi:10.4155/fsoa-2017-0003

[42] Nagashima, Jennifer B et al. "Evaluation of an ovary-on-a-chip in large mammalian models: Species specificity and influence of follicle isolation status." *Journal of tissue engineering and regenerative medicine* vol. 12,4 (2018): e1926-e1935. doi:10.1002/term.2623

[43] Talmadge, James E et al. "Murine models to evaluate novel and conventional therapeutic strategies for cancer." *The American journal of pathology* vol. 170,3 (2007): 793-804. doi:10.2353/ajpath.2007.060929

[44] Gallo, James M. "Pharmacokinetic/ pharmacodynamic-driven drug development." *The Mount Sinai journal of medicine, New York* vol. 77,4 (2010): 381-8. doi:10.1002/msj.20193

Group Member Contributions:

Team 1 group members contributed equally to this proposal. Below are specific roles of each member:

- Concept generation: ALL
- Specific Aims: ALL
- Significance, background, and innovation: ALL
- Approach, Aim #1: Adrian
- Approach, Aim #2: Lexi
- Approach, Aim #3: Yunqi
- Approach, Aim #4: Kanishka
- References: ALL
- Formatting, revisions: ALL

By typing our names below, we agree to submit this proposal.

- Lexi Bounds
- Adrian Lopez
- Yunqi Yang
- Kanishka Patel